Epidermal Growth Factor Receptor Internalization Rate Is Regulated by Negative Charges near the SH2 Binding Site Tyr992†

Michael R. Holbrook,[‡,§,||] John B. O'Donnell, Jr.,[§] Linda L. Slakey,[⊥] and David J. Gross*[,‡,§]

Program in Molecular and Cellular Biology, Department of Biochemistry and Molecular Biology, and College of Natural Sciences and Mathematics, University of Massachusetts at Amherst, Amherst, Massachusetts 01003

Received January 26, 1999; Revised Manuscript Received April 19, 1999

ABSTRACT: This study examines the effects of mutations at and in the vicinity of tyrosine 992 of the epidermal growth factor receptor (EGFr) on epidermal growth factor- (EGF-) stimulated internalization of the receptor. Two regions of the EGFr adjacent to this domain have been defined previously as internalization domains. The present work shows that the mutation of negatively charged amino acid residues near Tyr992 to their uncharged analogues increases the rate of EGF receptor internalization. In addition, the conversion of Tyr992, which is an EGFr ligand-induced autophosphorylation site, to phenylalanine also increases the rate of receptor internalization. However, the mutation of Tyr992 to a glutamate residue does not alter the receptor internalization rate. In addition, the truncation of the EGFr at glutamate 996 reduces the internalization rate by half. This result confirms previous reports that residues immediately C-terminal to Glu996 are necessary to allow the normal rate of ligand-induced receptor endocytosis. The data suggest that negative charge in the vicinity of Tyr992, and potentially the phosphorylation of the EGFr at Tyr992, reduces the rate of ligand-induced receptor endocytosis. This reduction in internalization rate increases the lifetime of the activated EGFr in the plasma membrane by about 70%, thus suggesting that phosphorylation of Tyr992 acts to increase the signaling capacity of the EGF receptor even as it directly acts as an SH2 binding site.

The epidermal growth factor receptor (EGFr)[1] is a 170 kDa single-pass transmembrane glycoprotein member of the receptor tyrosine kinase family. When cells expressing the EGFr are stimulated with EGF, they undergo a number of physiological responses. One of these is the clustering of receptors into clathrin-coated pits and subsequent internalization of the ligand-bound receptors. The aggregation of receptors occurs rapidly and receptors can be detected inside cells within 5 min of stimulation (*1*).

Two regions of the intracellular domain of the EGFr have been identified as internalization sequences. The first encompasses approximately residues 972−984 (*2*). Within this region is the binding site for the AP-2 adaptor protein complex (*3*, *4*). Following activation of the receptor, the AP-2 complex has been shown to bind to tyrosine 974 within the ^{973}FYRAL recognition sequence of the receptor (*4*). Also potentially involved in this association is Eps15, a protein that is phosphorylated following ligand activation of the EGFr and that colocalizes in coated pits with AP-2 (*5*). Phosphorylation of Eps15 also appears to be required for proper internalization of the EGFr (*5*).

The second internalization sequence has been identified as residues 996−1010 (*2*). This region contains a known internalization motif, ^{996}QQGFF, that is required for efficient internalization of the EGFr (*3*).

EGFr kinase activity is required for ligand-induced receptor internalization (*6*, *7*) and for sequestration of the EGFr into coated pits (*8*). In contrast, constitutive receptor internalization does not require ligand binding or activation of the receptor tyrosine kinase (*7*). Activation of the EGFr leads to receptor autophosphorylation as well as phosphorylation of other substrates. Receptors with inactive kinases are not efficiently recruited to coated pits for internalization (*7*, *8*).

Ligand activation and a functional kinase are required for the association of EGFr with adaptor proteins (*8*, *9*). The adaptor protein complex AP-2 consists of four proteins, two large (α and either β_1 or β_2), one medium (μ_2), and one small (σ_2) (*10*). The AP-2 complex associates with the EGFr through its μ chains (*10*, *11*) at Tyr974 of the EGFr within the ^{973}FYRAL binding motif (*3*, *4*). This association occurs at an approximately 1:1 stoichiometric ratio (*12*). Phosphorylation of the EGFr at Tyr974 is not required for AP-2

† These studies were supported in part by American Cancer Society Grant FRA-437 and National Science Foundation Grant MCB-9304393 (to D.J.G.). Any opinions, findings, and conclusions or recommendations expressed in this material are those of the authors and do not necessarily reflect the views of the funding organizations.

* To whom correspondence should be addressed: Department of Biochemistry and Molecular Biology, Lederle GRC, University of Massachusetts, Amherst, MA 01003-4505. Voice (413) 545-3170; Fax (413) 545-3291; Email dgross@biochem.umass.edu.

‡ Program in Molecular and Cellular Biology

§ Department of Biochemistry and Molecular Biology.

|| Present address: Department of Pathology, University of Texas Medical Branch, Galveston, TX 77555-0609.

⊥ College of Natural Sciences and Mathematics.

[1] Abbreviations: EGFr, epidermal growth factor receptor; EGF, epidermal growth factor; PLCγ, phospholipase Cγ; CHO, Chinese hamster ovary; PCR, polymerase chain reaction; FBS, fetal bovine serum; G418, geneticin; PBS, phosphate-buffered saline; BSA, bovine serum albumin; HEPES, 4-(2-hydroxyethyl)-1-piperazineethanesulfonic acid; PMSF, phenylmethanesulfonyl fluoride.

10.1021/bi990195r CCC: $18.00
Published on Web 06/24/1999

recognition, though the presence of receptor autophosphorylation sites does appear to be required for AP-2 association (*9*). Removal of the AP-2 binding sequence does not significantly affect receptor internalization (*13*). Thus, the role of AP-2 appears to be more as a recruitment tool as opposed to a direct mediator of receptor internalization.

Eps15, which is a phosphorylation substrate for the EGFr (*14*), binds to the α subunit of the AP-2 complex in an EGF-dependent manner (*5*). Eps15 and AP-2 colocalize with clathrin in coated pits and vesicles (*5*). EGF stimulation leads to the phosphorylation of Eps15 and the recruitment of the EPs15/AP-2 complex to the EGFr (*14*). The interaction of Eps15 with the AP-2 complex is required for EGFr endocytosis (*15*). This leads to the suggestion that the kinase activity of the EGFr is required for the phosphorylation of Eps15, which then mediates the association of the AP-2 complex with EGFr and subsequent association with clathrin.

Between the two internalization sequences lies the putative actin-binding domain of the EGFr, residues 984−996 (*16*). This domain, which is homologous to the α-helical actin-binding domain of *Acanthamoeba* profilin (*16*), has been identified on the basis of peptide competition (*16*) and mutagenic deletion of this domain (*17*). Within this domain lies Tyr992, which is the most N-terminal of the autophosphorylation sites of the EGFr (*18*). The phosphorylation of Tyr992 generates an SH2 binding domain that is a potential association site for a number of SH2-containing molecules, in particular phospholipase Cγ (PLCγ). Also within the putative actin binding domain are several negatively charged residues, all of which would present themselves at the surface of the cytoplasmic domain of the EGFr if the actin-binding domain were α-helical. A goal of the present work was to examine the role of the negative charges in the vicinity of Y992 on the rate of ligand-induced internalization of the EGFr.

Several point mutations were made in the putative actin-binding domain of the EGFr. These mutant EGFr were expressed in Chinese hamster ovary cells and were shown to possess tyrosine kinase activity. All point mutant EGFr involving a loss of negative charge within the actin-binding domain display an enhancement of their EGF-stimulated internalization rates. Quantitative analysis suggests that negative charge near Tyr992, and thus autophosphorylation of the EGFr at Tyr992, serves to slow the rate of receptor internalization and, consequently, reduces clearance of activated EGFr from the cell surface.

EXPERIMENTAL PROCEDURES

Cell Lines. Chinese hamster ovary cells (CHO-K1), A431 cells, and hybridomas expressing the 528 antibody were purchased from the American Type Culture Collection (Rockville, MD). CHO cells expressing the wild-type EGFr were a gift from Roger Davis at the University of Massachusetts Medical Center, Worcester, MA (*19*, *20*). The hybridoma cell line for the EGFR1 antibody was a gift from Michael Waterfield at the Imperial Cancer Research Fund Laboratories, London, England (*21*).

Construction of Mutant EGF Receptor Gene. The *Xba*I site of the *Xba*I−*Hind*III fragment of pXHER (*19*, *22*), which contains the human EGFr coding sequence, was converted to a *Sal*I site and the *Sal*I−*Hind*III fragment was cloned into pBK-CMV (Stratagene, La Jolla CA). This plasmid was designated pCMV-EGFr. Mutagenesis was performed by using the PCR overlap extension technique (*23*, *24*). Complementary mutant oligonucleotides were homologous to the 20 nucleotides surrounding the site of mutation. Flanking oligonucleotides were designed to be 5′ of the internal EGFr *Bgl*II site and 3′ of the *Hind*III site. Primary reactions were carried out with pCMV-EGFr as a template and appropriate combinations of flanking and mutant primers to generate PCR products that overlapped at the region of the mutant oligonucleotides. Secondary reactions were performed with the flanking primers and the products from the primary reaction as the template. The product from the second reaction resulted in an EGFr sequence with the proper mutations incorporated. The final PCR products were digested with *Bgl*II and *Hind*III and cloned into pCMV-EGFr from which the analogous wild-type sequence was removed. The PCR product sequence fidelity was confirmed by sequencing. Five mutant sequences were generated: Asp988 to Asn988 (D988N), Glu991 to Gln991 (E991Q), Tyr992 to Phe992 (Y992F), Tyr992 to Glu992 (Y992E), and Glu991 to Gln991 with null mutation at Gln997 (E991Qt$_{996}$).

Cell Culture. CHO cells do not express endogenous EGFr and thus were an excellent choice for expression of EGFr for these studies. All CHO cell lines were maintained in Hams/F12 nutrient medium (Gibco, Grand Island, NY) supplemented with 5% fetal bovine serum (FBS; Summit Biotechnology, Ft. Collins, CO) (complete medium). A431 cells, which are a human epidermoid carcinoma cell line, were used as a control as they endogenously express about 1×10^6 EGFr on their cell surface. These cells were maintained in Dulbecco's modified Eagle's medium (Gibco, Grand Island, NY) with 5% FBS. All cells were maintained in a humidified 37 °C incubator with 5% CO_2.

Transfection of Chinese Hamster Ovary Cells. pCMV-EGFr mutant plasmids Y992F, D988N, E991Q and E991Qt$_{996}$ were transfected into CHO-K1 cells via electroporation with an Invitrogen electroporator II (Invitrogen, Carlsbad, CA) following the manufacturer's instructions for electroporation of CHO cells. The Y992E mutants were transfected into CHO-K1 cells with the lipofection reagent CellFECTIN (Gibco, Grand Island, NY) following the manufacturer's instructions. Following transfection, cells were allowed to grow for 2−3 days and then were trypsinized and plated on 96-well tissue culture plates at a density of 10 cells (50 μL)$^{-1}$ well^{-1} in selection medium (complete medium with 400 μg/mL G418; Gibco, Grand Island, NY). Twenty-four hours later, 200 μL of additional selection medium was added and the cells were incubated for about 2 weeks or until colonies were readily apparent. Cells from individual wells of the 96-well plates were trypsinized and transferred to 35 mm dishes for expansion for 2−3 days. The cells were then plated on glass cover slips for immunofluorescence screening (below). Cells that screened positive were plated on 96-well plates at a density of <1 cell (50 μL)$^{-1}$ well^{-1} for secondary cloning. Cell cultures were fed an additional 200 μL of selection medium 24 h later and incubated for 2 weeks. The cells were checked again for expression by use of fluorescence microscopy to determine expression levels. The single cell cloning was performed a second time and cells were screened for homogeneous high receptor expression.

Mammalian Cell Screening for Receptor Expression. Epidermal growth factor receptor transfected cells were screened for EGFr expression levels by use of fluorescent antibody detection on fixed cells. Cells were plated onto glass

cover slips and grown in complete medium for 3 days. Cells were washed three times with PBS and fixed for 10 min at room temperature with 4% paraformaldehyde in PBS, followed by two washes with PBS. The cells were incubated in blocking buffer (0.1% BSA in PBS) for 30 min at room temperature, followed by a 1 h incubation with primary antibody [either mAb EGFR1 or 528 (*21*, *25*)] at a concentration of 20 μg/mL in blocking buffer. The cells were washed three times with PBS and incubated for 1 h at room temperature with the appropriate secondary antibody at 1 μg/mL diluted in blocking buffer. The cover slips were then washed once with PBS, mounted on glass slides in PBS:glycerol (1:1), and sealed with clear nail polish. Control cells were treated identically except that the primary antibody was left out of the procedure.

Phosphorylation Assay. This assay was derived from an experiment presented by Livneh et al. (*26*). EGF receptor-expressing CHO cells or A431 cells were plated at a density of 1×10^6 cells per 100-mm dish and grown in complete medium for 3 days. Generally two dishes were used for each test on a particular cell line. The cells were washed twice with PBS and incubated with serum-free medium for about 24 h. The cells were harvested in 2 mL of PBS by scraping with a rubber policeman. The cells were pelleted (600*g*, 5 min) and resuspended in HNEG buffer (50 mM HEPES, pH 7.5, 150 mM NaCl, 1 mM EDTA, 10% glycerol, 1% Triton X-100, 10 μg/mL aprotinin, 1 mM PMSF, 20 mM benzamidine, and 10 μg/mL leupeptin) and incubated on ice for at least 45 min. Protein A−Sepharose beads (Sigma Chemical Co., St. Louis, MO), about 30 μL/immunoprecipitation, were washed three times in 200 mM HEPES, pH 7.5, and incubated with 1 μg of Ab/10 μL of beads in 200 mM HEPES, for 1 h at 4 °C on a rotator. The beads were washed three times with buffer B (20 mM HEPES, pH 7.5, 150 mM NaCl, 10% glycerol, and 0.1% Triton X-100). The cell lysates were centrifuged in a microcentrifuge at top speed for 3 min to remove the insoluble fraction and the supernatants were added to the beads and incubated at least 1 h at 4 °C on a rotator. Following the incubation with cell lysates, aliquots of beads were taken at 10 μL of beads per each of two tubes per sample. The first tube was tested for EGF-stimulated activity and the second for unstimulated activity. Following immunoprecipitation, phosphorylation stock solution {333 μM (3 μCi) [γ-^{32}P]dATP (Amersham, Arlington Heights, IL), 50 mM $MnCl_2$, and 15 mM angiotensin II (Sigma Chemical Co., St. Louis, MO)} was diluted 1:9 in buffer B and 20 μL was added to the beads. EGF-stimulated tubes included 16.4 nM (100 ng/mL) EGF (Harlan Bioproducts, Indianapolis, IN) final concentration in the phosphorylation buffer. The reactions were allowed to proceed on ice for 10 min and lightly spun, and the supernatants were removed to clean tubes. Forty microliters of 1× Laemmli SDS−PAGE sample buffer were added to the beads, which were boiled for 4 min prior to running on an SDS−PAGE gel. The supernatant was spotted onto duplicate 2.1 cm phosphocellulose circles in 7.5 μL aliquots per circle. The circles were allowed to air-dry and then were washed three times for at least 15 min with 50 mM phosphoric acid to removed unincorporated [γ-^{32}P]dATP. The circles were placed in scintillation vials and 3 mL of Scintiverse E (Fisher Scientific, Pittsburgh, PA) was added. The samples were then counted on a Beckman scintillation counter with a window of 0−1000 keV. To measure nonspecific phosphorylation of angiotensin II, a control immunoprecipitaion of CHO-K1 cells lacking the EGFr was performed with each experiment. The value for phosphorylation in CHO-K1 cells was subtracted from the values obtained from each of the EGFr-expressing cell lines. Nonspecific angiotensin II phosphorylation in the CHO-K1 controls was 0.057 pmol/min.

Internalization Assay. This protocol is essentially as described by Theroux et al. (*27*). Cells were plated on 48-well plates at a density of 1×10^4 cells per well and grown for 3 days in complete medium. Cells were incubated with serum-free medium for 4−5 h prior to initiation of the experiment. Immediately prior to initiation of the experiment, three wells were treated with trypsin and the cells were counted. Following trypsinization the plate containing the cells to be treated was placed in a water bath, which was held at a constant 37 °C, and allowed to equilibrate for 5 min. The cells were then treated with 16.4 nM EGF {5 ng/mL ^{125}I-EGF (Amersham, Arlington Heights IL) and 95 ng/mL unlabeled EGF} in a volume of 50 μL for a specified period of time. All tests were carried out in triplicate wells. Cells were treated for 0, 2, 4, 8, 12, 20, and 30 min and the stimulation was carried out in reverse order so that all cells could be chilled simultaneously. At the end of the incubation period, the plate was put on ice and 250 μL of ice-cold PBS was added immediately to each well. The PBS washes were removed to individual 12 × 75 mm polypropylene tubes. This wash was repeated and combined with the first and counted as the unbound fraction. The plasma membrane-associated ^{125}I-EGF was removed with a 3 min, 250 μL ice-cold acid wash (50 mM NaCl and 150 mM glycine, pH 3.0). The acid wash and a subsequent PBS wash were collected and counted as the membrane-bound fraction. The cells were then solubilized with cold 0.62 N NaOH for about 5 min. The NaOH was removed and the wells were washed once with PBS. The NaOH and PBS wash were counted together as the internalized fraction. Samples were counted for 5 min in a Beckman Gamma 5500B γ counter with a window of 0−36 keV. All polypropylene tubes contained at least 1 mL of water prior to any solution additions to ensure sufficient volume for efficient counting in the γ counter. Standard curves were generated for each batch of ^{125}I-EGF and the amount of EGF in each fraction was calculated on the basis of the counts in each fraction, the standard curve, and the 19:1 dilution factor.

Internalization Modeling. To quantify the differences in internalization between the mutant receptors and the wild-type receptors, a very simple internalization model was developed following the procedures of Wiley, Lauffenburger, and colleagues (*7*, *28*). This model utilizes only two steps, ligand import and ligand export. The rates for both of these processes were assumed to be constant and the two processes were assumed to follow first-order reaction kinetics. From these assumptions, rate equations were developed. These functions fit the data reasonably well. The two rate constants in the model are employed as variable parameters in Marquardt−Levenberg nonlinear least-squares fits to the data. The first (k_e) is the internalization rate constant, while the second (k_p) accounts for the loss of ligand due to postinternalization processing, assumed to be through ligand export from the cell, either via degradation or recycling release. The processing rate constants for recycling (k_x) and degradation (k_h) have been lumped together in this way in previous modeling of EGFr internalization (*7*).

The rate equation governing EGF internalization based on this model is

$$\frac{dC_i}{dt} = k_e C_s - k_p C_i \quad (1)$$

where k_e and k_p are defined as above and C_i and C_s are the amounts of EGF internalized and bound to the cell surface, respectively. The solution to this equation relating internalized EGF to surface-bound EGF is

$$C_i = k_e I e^{-k_p t} \quad (2)$$

where

$$I = \int_0^t C_s(t') e^{k_p t'} \, dt' \quad (3)$$

To implement the fit of the data to this model, the surface-bound EGF versus time data were first fit to an empirical two-exponential function that provided a well-fit analytical expression for C_s. This analytical expression was then employed to calculate C_i from eqs 2 and 3, which was then fit to the internalization data. All fitting was done with the IGOR data analysis program (WaveMetrics, Lake Oswego, OR).

A second, more physiologically complete model for EGFr internalization was examined. This model, a simplified version of one similar to that presented by Starbuck and Lauffenburger (*29*) and Sorkin et al. (*30*), included concentrations of free (C_r) and ligand-bound (C_s) EGFr on the cell surface, concentrations of free (C_x) and ligand-bound (C_i) internalized EGFr, the concentration of free EGF (L) in the bathing medium, the concentration of intracellular free EGF (L_i), a (constant) velocity of replacement of EGFr to the cell surface (V), and rate constants for binding (k_f) and dissociation (k_r) of EGF with cell surface EGFr, endocytosis of ligand-occupied surface EGFr (k_e), recycling of internalized, occupied EGFr (k_x), dissociation of EGF from internalized, occupied EGFr (k_d) and export of internalized, degraded EGF from the cell (k_h). The values of k_f and k_r were constrained such that k_r/k_f was held constant at values for the dominant, low-affinity equilibrium dissociation constant measured for each of the mutant EGFrs in other experiments. The differential equations describing this model system are

$$\frac{dC_r}{dt} = k_r C_s - k_f L C_r + V$$

$$\frac{dC_s}{dt} = k_f L C_r - k_r C_s - k_e C_s$$

$$\frac{dC_i}{dt} = k_e C_s - (k_d + k_x) C_i \quad (4)$$

$$\frac{dC_x}{dt} = k_d C_i$$

$$\frac{dL_i}{dt} = k_d C_i - k_h L_i$$

where the variables and constants are as given above. The solutions of these equations for surface-bound and internalized EGFr are, respectively and

$$C_s = R_T \frac{k_f L}{\kappa_2 - \kappa_1}(e^{-\kappa_1 t} - e^{-\kappa_2 t}) + \frac{V}{k_e(\kappa_2 - \kappa_1)}\{\kappa_2(1 - e^{-\kappa_1 t}) - \kappa_1(1 - e^{-\kappa_2 t})\} \quad (5)$$

$$C_i = \frac{1}{(k_d + k_x - \kappa_1)(k_d + k_x - \kappa_2)}\left\{R_T k_f k_e L\left[e^{-(k_d + k_x)t} + \frac{k_d + k_x - \kappa_2}{\kappa_2 - \kappa_1} e^{-\kappa_1 t} - \frac{k_d + k_x - \kappa_1}{\kappa_2 - \kappa_1} e^{-\kappa_2 t}\right] + V\left[\frac{k_f k_e L}{k_d + k_x}(1 - e^{-(k_d + k_x)t}) + \frac{(k_d + k_x - \kappa_2)\kappa_2}{\kappa_2 - \kappa_1}(1 - e^{-\kappa_1 t}) - \frac{(k_d + k_x - \kappa_1)\kappa_1}{\kappa_2 - \kappa_1}(1 - e^{-\kappa_2 t})\right]\right\} \quad (6)$$

where R_T is the total amount of EGFr on the cell surface at $t = 0$,

$$\kappa_1 = \frac{k_e + k_r + k_f L + [(k_e + k_r + k_f L)^2 - 4k_f k_e L]^{1/2}}{2}$$

and

$$\kappa_2 = \frac{k_e + k_r + k_f L - [(k_e + k_r + k_f L)^2 - 4k_f k_e L]^{1/2}}{2}$$

A more complicated expression for L_i, which includes dependence on the ligand degradation rate k_h, is not shown here.

To implement the fit of the data to this model, the surface-bound EGF versus time data were first fit to eq 5 allowing k_r, k_e, V, and R_T to vary. The equation for the predicted total internalized ligand ($C_i + L_i$) was then fit against the measured internalized EGF data holding k_r, k_e, V, and R_T fixed and allowing k_d and k_x to vary.

A second fitting scheme for the more complicated model was also employed. The integral of C_s (eq 5) was computed as for the simple model. Data in the form of actual internalized EGF versus the integral of actual surface-bound EGF was used to fit the theoretical curve. Because it was not possible to solve the equation for total internal EGF ($C_i + L_i$) in terms of the integral of C_s in closed form, an iterative approach was used to first compute t, the time at which the integral of C_s reached its input value, to 0.1% accuracy. This value was then used to compute $C_i + L_i$ to complete the evaluation of the function. All fitting was done with the IGOR data analysis program (WaveMetrics, Lake Oswego, OR).

RESULTS

Kinase Activity. The four point mutants and one truncation mutant EGFr were assayed for Tyr kinase activity along with WT EGFr expressed in CHO cells. Immunoprecipitated, purified EGFr were incubated with [γ^{32}P]ATP and levels of autophosphorylation, as well as exogenous substrate phosphorylation, were measured. Analysis of receptor autophosphorylation by SDS−PAGE autoradiography clearly indicates that all of the receptors, with the exception of

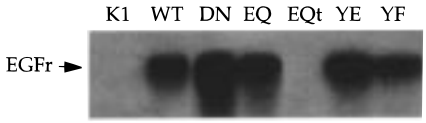

FIGURE 1: EGFr kinase activity. CHO cells expressing wild-type and mutant EGFr were solubilized and the EGFr was immunoprecipitated with receptor-specific mAb EGFR1. Phosphorylation assays were carried out on the immunoprecipitated receptors in the presence of [γ-^{32}P]ATP and angiotensin II. The immunoprecipitated receptors were treated with 1× sample buffer and run on SDS−PAGE. The receptors are seen as a single band with a molecular mass of 170 kDa. The control untransfected CHO-K1 parental line (K1) as well as the truncation mutant E991Qt$_{996}$ line (EQt) show no phosphorylated receptor. The wild-type (WT), D988N (DN), E991Q (EQ), Y992E (YE), and Y992F (YF) cell lines all show receptor autophosphorylation. The lower molecular weight band of the truncation mutant E991Qt$_{996}$ would be off the gel image shown, but no band was detected in the original gel. Western blot analysis confirmed the presence of EGFr in all lanes except that for the CHO-K1 line (not shown).

Table 1: Relative Kinase Activity[a]

cell line	pmol/min
wild type	0.030
D988N	0.024
E911Q	0.054
E911Qt$_{996}$	0.020
Y992E	0.052
Y992F	0.044

[a] The reaction supernatant from the phosphorylation assays was removed from the immunoprecipitates following the reaction and was spotted on phosphocellulose circles. The level of angiotensin II phosphorylation is reported as a relative measure of kinase activity. Nonspecific activity from paired control immunoprecipitates from CHO-K1 cells that are devoid of EGFr was subtracted from the data.

E991Qt$_{996}$, are able to autophosphorylate (Figure 1). These assays were performed with receptor-specific immunoprecipitates from receptor-expressing CHO cell lysates. The ^{32}P-labeling of receptors can be seen as a band of about 170 kDa. Neither the CHO-K1 cells, which do not express EGFr, nor the E991Qt$_{996}$ cells demonstrate any detectable level of EGFr autophosphorylation. The lack of phosphorylation of the E991Qt$_{996}$ mutant is due to the elimination of four of the five tyrosine autophosphorylation sites plus the likely elimination of the fifth site at Tyr992 due to the loss of the negative charge at Glu991 (*31*, *32*). In these assays cells were treated in both the presence and absence of EGF with little variation in the level of EGFr autophosphorylation (data not shown). This result suggests that the receptor is in an activated state in the immunoprecipitates; this effect with mAb R1 has previously been reported (*33*). What is clear from the results here is that all mutant EGFr except the E991Qt$_{996}$ truncation mutant can autophosphorylate.

Receptor kinase activity as measured by the ability to phosphorylate angiotensin II, an exogenous substrate, was assayed in order to demonstrate the activity of all EGFr mutants. These experiments were performed on immunopurified EGFr with a limiting amount of antibody so that the amount of EGFr was approximately the same in all assays. The relative kinase activity was similar for all receptor mutants, including E991Qt$_{996}$, and the wild-type receptor (Table 1). This result demonstrates that all mutant EGFr express active tyrosine kinase activity, and thus the lack of autophosphorylation of E991Qt$_{996}$ is due to the loss of tyrosine phosphorylation sites as suggested above. All mutant EGFr nevertheless express competent tyrosine kinase domains.

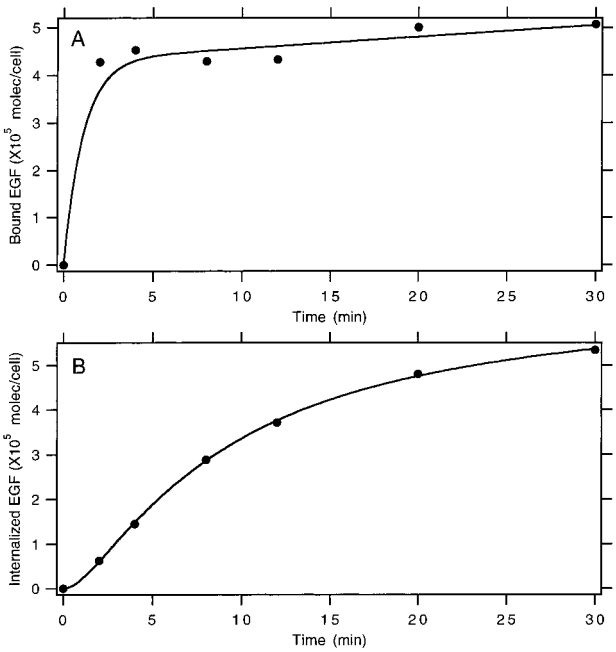

FIGURE 2: Internalization of wild-type EGFr. Serum-starved CHO cells expressing the wild-type EGFr were treated with 16.4 nM EGF, 0.82 nM of which was ^{125}I-EGF. Internalization data were fit by a simple two-step internalization model. Data for (A) surface-bound EGF versus time and (B) internalized EGF versus time are plotted over the 30 min course of the experiment. Fits of the internalization model to the data are shown by the smooth curves.

Receptor Internalization. Given that the five mutant EGFr studied here are functional as kinases, the role of negative charges in the vicinity of Tyr992 in modulation of internalization of the receptor was examined. The internalization of ^{125}I-EGF was measured in each of the mutant EGFr-expressing CHO cell lines as well as wild-type receptor-expressing CHO cells and A431 cells. The data generated from these experiments were analyzed by using a simple kinetics model for the endocytic process to fit the data. The model included only an endocytosis step and a step involving recycling release or degradative loss of ligand from the cell.

The internalization of ^{125}I-EGF for wild-type EGFr-expressing CHO cells is shown as an example; results are qualitatively similar for all cell lines tested. The cells show near-maximal ligand binding within 5 min of addition of ^{125}I-EGF (Figure 2A). The internalization of ligand does not appear to be saturable within the time frame of the experiment, as shown by plotting the amount of ligand internalized versus time (Figure 2B). To calculate the rate of receptor internalization, the data for all cell lines were plotted as the internalized ligand versus the time integral of surface-bound EGF in a plotting method developed by Lund et al. (*28*) (Figure 3). The slope in the linear portion of this plot corresponds to the net rate of internalization so long as internalization dominates over ligand processing and release. At the onset of internalization this appears to be the case, but at the later stages of internalization the plot clearly deviates from linearity, which demonstrates that internalization of ^{125}I-EGF in these WT receptor-expressing cells is more than a one-step process. The downward curvature of the plot shows that the net internalization rate declines as

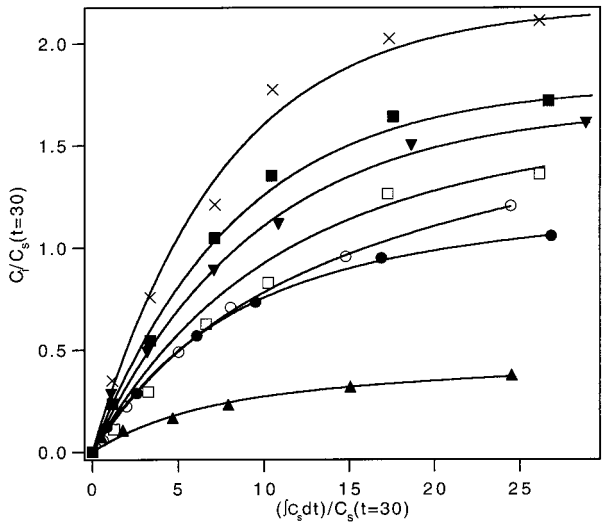

FIGURE 3: Internalization of mutant and wild-type EGFr. Cells expressing wild-type (WT and A431) or mutant EGFr were assayed for receptor internalization. Cells were treated with 16.4 nM EGF, 0.82 nM of which was ^{125}I-EGF. Internalization and surface binding of ^{125}I-EGF was followed for 30 min. The data from CHO cells expressing wild-type EGFr (●) and A431 cells (○) along with D988N (▼), E991Q (×), E991Qt$_{996}$ (▲), Y992E (□), and Y992F (■) EGFr-expressing CHO cells were fit to a two-step internalization model (smooth curves). To present all data on the same plot, each data set and its fit have been normalized to the fitted value of cell surface associated ^{125}I-EGF at $t = 30$ min. The abscissa plots the time integral of surface-bound ^{125}I-EGF, while the ordinate plots the internalized ^{125}I-EGF. A plot of this nature should give a straight line if the internalization process follows a single internalization step; the downward curvature indicates that the net rate of ^{125}I-EGF internalization diminishes with increased internalization of ligand. The two-step internalization model fits the data reasonably well. The point mutants are given by their single amino acid codes. The E991Qt$_{996}$ mutant is truncated at residue Glu996.

total internalized EGF increases, which suggests that EGFr processing after internalization leads to loss of EGF from the cell. The data from the wild-type and mutant receptor-expressing CHO cell lines and A431 cells show qualitatively similar results when plotted in this manner (Figure 3). A linear regression fit of the data points deriving from early times (≤5 min post-EGF) for each data set was examined. The internalization rate constant values, derived from the slopes of the C_i versus integrated C_s plots for each mutant and WT receptor, were consistently less than those obtained by fits to each whole set of data points. This suggests that processing of internalized EGFr under the conditions employed in these experiments is sufficiently rapid that it cannot be excluded from analysis, even for times as short as 5 min.

Examination of the internalization rates derived from this fitting procedure (Table 2) demonstrates that the rates for the wild-type receptor as expressed on the surface of either A431 or CHO cells and the Y992E mutant are approximately the same (0.134, 0.139, and 0.15 min^{-1}, respectively). The E991Qt$_{996}$ receptor is internalized at a rate about half that of the wild-type receptor, 0.06 min^{-1}, similar to other C-terminal truncation mutants (*2*, *30*, *34*, *35*). The Y992F, E991Q, and D988N mutants have increased internalization rates of 0.22, 0.29, and 0.18 min^{-1}, respectively. The fact that these mutants internalize at an increased rate is interesting, as all three are potentially defective in phosphorylation at tyrosine 992. The Y992F mutant cannot be phosphorylated at this tyrosine residue due to the loss of the phenyl hydroxyl

Table 2: Internalization and Processing Rates of Wild-Type and Mutant EGF Receptors[a]

cell line (*n*)	k_e (min^{-1})	k_p (min^{-1})	$C_{s,t=30}$(×10^5/cell)
wild type (4)	0.139 ± 0.002	0.112 ± 0.003	5.05
A431 (3)	0.134 ± 0.005	0.096 ± 0.005	40.30
D988N (3)	0.18 ± 0.01	0.107 ± 0.009	1.28
E991Q (4)	0.29 ± 0.02	0.13 ± 0.01	1.28
E991Qt$_{996}$ (3)	0.06 ± 0.01	0.14 ± 0.03	1.27
Y992E (4)	0.15 ± 0.01	0.10 ± 0.01	5.62
Y992F (3)	0.22 ± 0.01	0.121 ± 0.005	2.57

[a] Data pooled from three or more separate experiments were fit to a two-step internalization model. The ligand internalization (k_e) and loss (k_p) rates were calculated as described in the text. The uncertainties in the parameters as estimated by the curve-fitting routine are also shown. The total number of receptors (C_s) expressed on the cell surface at the end of the assay ($t = 30$ min) is given for each of the cell lines. The point mutants are given by their single amino acid codes. the E991Qt$_{996}$ mutant is truncated at residue Glu996.

on the amino acid side group. The E991Q and D988N mutants may be phosphorylation-deficient as the negative charges at these positions are important for kinase recognition (*31*, *32*).

The ligand processing and export rates based on the simple two-step model are found to be approximately the same for all of the receptors. The rates range from 0.096 to 0.14 min^{-1}. These values are somewhat faster than those found for wild-type EGFr expressed in B82 mouse L-cells (*7*, *36*) and kinase-inactive EGFr expressed in B82 mouse L-cells (*37*) but are less than the recycling rate constant for EGFr truncated at residue 647 expressed in B82 mouse L-cells (*37*). These rates, which reflect processing of the internalized EGFr, thus appear to be insensitive to mutations that alter the charge near Tyr992 or its ability to be phosphorylated.

A more complex model of EGF internalization similar to those of Starbuck and Lauffenburger (*29*) and Sorkin et al. (*30*) was examined. This model contained seven free parameters to fit. Two approaches were used to fit the model to the internalization data as described in Materials and Methods, and both produced satisfactory fits as judged by eye (not shown). The uncertainty in the parameter fit values, however, was very large, indicating that the models were insufficiently constrained to provide accurate fits to the data. The internalization rate constants for all mutant and WT EGFr obtained from the model fits are shown in Table 3 along with their corresponding uncertainties. The internalization rates are in reasonable agreement with those found from the simple model, particularly in that the relationship among different mutants and WT EGFr is found by either modeling scheme. The rate constants of steps after the internalization step for the more complicated model displayed similarly large uncertainties. Because the fits did not return satisfactorily characterized rate constants, more physiologically accurate models were not further analyzed.

DISCUSSION

This study examines the role of negatively charged amino acid residues in the vicinity of Tyr992, the most N-terminal autophosphorylation site of the EGFr, in modulating ligand-induced EGFr internalization. This region has previously been shown to bridge two key internalization regulation domains and has been suggested to be a region at which the EGFr interacts with actin. Four point mutations have been

Table 3: Internalization Rates of Wild-Type and Mutant EGF Receptors Obtained from the More Complicated Internalization Scheme[a]

cell line (*n*)	k_e (min^{-1}) two-step fit	k_e (min^{-1}) integral fit
wild type (4)	0.094 ± 0.096	0.11 ± 73
A431 (3)	0.088 ± 0.040	0.11 ± 2000
D988N (3)	0.17 ± 0.35	0.18 ± 170
E991Q (4)	0.21 ± 0.28	0.27 ± 37
E991Qt$_{996}$ (3)	0.06 ± 0.04	0.053 ± 1.5
Y992E (4)	0.074 ± 0.013	0.092 ± 250
Y992F (3)	0.13 ± 0.23	0.18 ± 23

[a] Data pooled from three or more separate experiments were fit to an internalization model that included steps for the kinetics of ligand association, internalization, and subsequent processing. The model was fit to the data as described in the text. Two fitting schemes were employed; one (two-step fit) first fit the surface-bound ligand data and then fit the internalization data, while the second (integral fit) fit the internalization data as a function of the integral of the surface-bound ligand data. The internalization rate constant (k_e) is shown along with its estimated uncertainty. The point mutants are given by their single amino acid codes. The E991Qt$_{996}$ mutant is truncated at residue Glu996.

made within this domain that alter its charge characteristics and, additionally, the phosphorylation competence of Tyr992. The results from this work suggest that negative charges in this region, and possibly the phosphorylation of Tyr992, are important for regulating the internalization rate of the EGFr. A truncation of the EGFr at Glu996 has confirmed that the role of the C-terminus, including the ^{996}QQGFF internalization motif, is significant in regulating the ligand-induced receptor internalization rate.

Values for k_e, the internalization rate constant, obtained for WT EGFr expressed in A431 cells and CHO cells, 0.14 min^{-1}, are somewhat higher than the value found in WT EGFr expressed in B82 mouse L-cells (0.09 min^{-1}; ref *7*). This difference possibly reflects the differing cell backgrounds. CHO cells that express the D988N, E991Q, and Y992F mutant receptors have higher rates of EGF-induced receptor internalization than do wild-type receptor-expressing cells (Table 2). The D988N mutant internalizes at 0.18 min^{-1}, while the E991Q and Y992F mutants internalize even faster at 0.29 and 0.22 min^{-1}, respectively. These data suggest that negative charge along the acidic face of the putative α-helix N-terminal to and including Tyr992 decreases the rate at which the EGFr internalizes. The D988N and E991Q mutations convert acidic residues to their uncharged analogues, while the Y992F mutation eliminates a site of tyrosine phosphorylation. The finding that the E991Q mutant receptors are internalized faster than the D998N and Y992F mutants is interesting because this mutation, in addition to eliminating the negative charge at position 991, may also prevent phosphorylation at Tyr992. Part of the tyrosine kinase target recognition motif includes the presence of several negatively charged residues immediately N-terminal to the target tyrosine (*31*, *32*). The potential loss of two negative charges by this mutation may enhance the effect of the single charge-neutralizing mutation. This suggests that phosphorylation at Tyr992 plays an important role in regulating the internalization of the EGFr and that the direct effect of the E991Q mutation adds to that due to phosphorylation loss. Prevention of phosphorylation at Tyr992, as is the result of the Y992F mutant, increases the rate of receptor internalization, as is consistent with this interpretation. The enhanced rate of receptor internalization in the E991Q mutant combined with the lesser increase in receptor internalization rate of the D988N mutant suggests that the presence of negative charges along the acidic face of the helix, applied additively to that due to receptor phosphorylation, act synergistically to inhibit the rate of internalization of the EGFr.

The Y992E mutant-expressing cell line has an internalization rate of 0.15 min^{-1}, which is similar to rates for WT EGFr expressed in CHO and A431 cells. This mutation will prevent phosphorylation at Tyr992 even as it confers a negative charge at this site. This mutation probably does not confer residue 992 with the ability to bind SH2-containing proteins with the same affinity as native EGFr pY992, since that interaction involves specific coordination of the phenyl ring and the phosphate with residues in the SH2 domain (*41*). However, peptide ligands that recognize SH2 domains do retain some affinity upon modification of their pTyr residues (*42*). Thus, the Y992E result suggests that phosphorylation of Y992, as would be occurring in the WT receptors in CHO and A431 cells, modulates the receptor internalization rate primarily due to the presence of additional negative charge rather than the presence of a phosphotyrosine residue at this site.

One mutant cell line studied here, E991Qt$_{996}$, internalizes EGFr at a rate that is slower than that for the wild-type receptors, 0.06 min^{-1}. This truncated mutant probably internalizes more slowly due to a loss of the ^{996}QQGFF internalization sequence (*3*). It is also possible that a deletion of this magnitude causes an alteration in the receptor conformation that obscures the AP-2 binding site at Tyr974. Similar effects due to EGFr C-terminal truncation have been seen previously (*2*, *34*), although a partial truncation at residue 1022 enhanced the internalization rate 50% over that of WT EGFr (*7*). An interesting aspect of the behavior of the E991Qt$_{996}$ truncation mutant is that the enhanced internalization seen for the complete E991Q mutant EGFr is completely reversed by the C-terminal 190 amino acid deletion. This demonstrates that the negative charges in the vicinity of Tyr992 that inhibit the EGFr internalization rate require the activity of the internalization domain of the EGFr C-terminal to residue 996, ^{996}QQGFF. The negative charges near Tyr992 may be required for direct interaction with parts of the internalization apparatus or may be required for structural integrity of the AP2 binding region surrounding Tyr974 of the EGFr.

The result that loss of phosphorylation on Tyr992 enhances the rate of internalization of the EGFr stands in contrast to the conclusion reached about this mutation when EGFr is expressed in 3T3 cells (*34*). In this cell system, a Y992F mutant EGFr internalized at a rate similar to that of WT EGFr. However, a Y992Ft$_{1063}$ truncation mutant internalized more slowly than a similar truncation mutant with WT sequence (*34*). These results suggest that the behavior of the EGFr in a 3T3 cell background is somewhat different than in a CHO cell background and that the presence of a phosphate on Tyr992 is irrelevant to EGFr internalization in 3T3 cells unless the C-terminal 123 amino acids of the receptor are truncated. In the latter case, the presence of a phosphate on Tyr992 appears to enhance the rate of receptor internalization. Although the differences between the present report and that of Sorkin et al. (*34*) are difficult to reconcile, they may lie in differences between cell lines in the presence

of cytosolic proteins with high affinity for the Tyr992 site.

The putative actin-binding domain of the EGFr, in which the mutations described in this paper were made, lies between the AP-2 binding domain and a second domain that has been identified as being required for EGFr endocytosis. The actin-binding domain was initially identified on the basis of its homology to the actin-binding domain of profilin from *Acanthamoeba*, which is known to be an α-helix (*16*, *38*, *39*). Computer modeling suggests that this domain within the EGFr also has the propensity to form a helix (not shown). A helical wheel diagram of this EGFr domain shows that the putative helix has two distinct faces. One face is largely hydrophobic and would likely abut another portion of the receptor. The other face is largely acidic in nature and includes the most N-terminal EGFr autophosphorylation site, Tyr992, as well as all of the sites of point mutation generated for this study. The crystal structure of the complex between *Yersinia* protein tyrosine phosphatase and a phosphohexapeptide of residues 988−993 of the EGFr (^{988}DADEpYL) suggests that the peptide N-terminal to Y992 is in a twisted β-sheet conformation with the remainder in an α-helical conformation (*40*). If this were the structure of this sequence in the native EGFr, Y992 and D988 would face one side of the β-sheet while E991 would face the opposite side.

Tyr992 and its surrounding amino acids form the binding locus for several different proteins that interact with the EGFr including actin, AP-2, and phospholipase Cγ (*43*−*46*). This region of the receptor, and thus its autophosphorylation residue Tyr992, defines a regulatory "hot spot" that is critical for at least three separate EGFr functions: internalization, cytoskeletal association and calcium signaling. Results presented here show that negative charges in this domain decrease the rate of ligand-induced internalization of the EGFr. The presence of these residues thus increases the lifetime of activated EGFr on the cell surface and therefore acts to enhance the signaling capacity of the EGFr. From the internalization rate constants obtained here, the WT EGFr has a half-life of 5 min after ligand binding, while the phosphorylation-incompetent Y992F mutant has a 3 min half-life. Phosphorylation of Tyr992 thus appears to function at least in part to increase the persistence of the activated EGFr at the plasma membrane by 70%, which would increase the signaling strength of the receptor by this amount. This result also suggests that the action of protein tyrosine phosphatases on pTyr992 would conversely decrease activated EGFr lifetime and signal strength. Thus, pTyr992 appears to act in an autoregulatory fashion to promote SH2 signaling molecule activation directly as well as to increase the signaling duration of this site at the plasma membrane.

Previous results from other laboratories have clearly demonstrated that kinase-inactive EGFr have a much reduced internalization rate as compared to WT EGFr (*7*, *34*, *37*), suggesting that tyrosine phosphorylation of the cytoplasmic domain of the receptor is necessary for efficient internalization. Our results suggest that the presence of negative charge in the vicinity of Tyr992, which would be enhanced by phosphorylation of Tyr992, slows the rate of internalization of the EGFr. Thus, it appears that multiple tyrosine phosphorylation events act as regulatory controls of receptor internalization, with some functioning to activate coated-pit-mediated endocytosis while others inhibit this pathway.

The inhibition of the rate of endocytosis by negative charges in the vicinity of Tyr992 suggests either that this domain interacts with molecules that modulate the efficiency of coated-pit-mediated internalization or that it acts allosterically to alter the conformation of portions of the receptor that are responsible for mediation of endocytosis. The latter is supported by the recent finding that phosphorylation of Tyr992 is necessary for a conformational shift of the EGFr between residues 979 and 1150 (*47*). Thus, increase in negative charge near Tyr992, including phosphorylation of Tyr992, may induce a conformational change that, in turn, may alter the interaction of the EGFr with the endocytic apparatus.

The former possibility is supported by findings that Tyr992 and residues near it interact with signal transduction components including PLCγ (*46*) and Src (*48*−*50*). Additionally, this domain has been suggested to be the site at which EGFr interacts with cytoskeletal F-actin (*16*). Presumably any interaction with proteins that bind near Tyr992 will sterically inhibit interactions of other molecules that bind nearby, including those that interact with the EGFr internalization sequences ^{973}FYRAL and ^{996}QQGFF.

REFERENCES

1. Sorkin, A., Waters, C. M. (1993) *BioEssays 15*, 375−382.
2. Chen, W. S., Lazar, C. S., Lund, K. A., Welsh, J. B., Chang, C.-P., Walton, G. M., Der, C. J., Wiley, H. S., Gill, G. N., and Rosenfeld, M. G. (1989) *Cell 59*, 33−43.
3. Chang, C.-P., Lazar, C. S., Walsh, B. J., Komuro, M., Collawn, J. F., Kuhn, L. A., Tainer, J. A., Trowbridge, I. S., Farquahr, M. G., Rosenfeld, M. G., Wiley, H. S., and Gill, G. N. (1993) *J. Biol. Chem. 268*, 19312−19320.
4. Sorkin, A., Mazzotti, M., Sorkin, T., Scotto, L., and Beguinot, L. (1996) *J. Biol. Chem. 271*, 13377−13384.
5. Tebar, F., Sorkina, T., Sorkin, A., Ericsson, M., and Kirchhausen, T. (1996) *J. Biol. Chem. 271*, 28727−28730.
6. Avruch, J., Zhang, X., and Kyriakis, J. M. (1994) *Trends Biochem. Sci. 19*, 979−983.
7. Wiley, H. S., Herbst, J. J., Walsh, B. J., Lauffenburger, D. A., Rosenfeld, M. G., and Gill, G. N. (1991) *J. Biol. Chem. 266*, 11083−11094.
8. Lamaze, C., and Schmid, S. L. (1995) *J. Cell Biol. 129*, 47−54.
9. Nesterov, A., Kurten, R. C., and Gill, G. N. (1995) *J. Biol. Chem. 270*, 6320−6327.
10. Ohno, H., Fournier, M. C., Poy, G., and Bonifacino, J. S. (1996) *J. Biol. Chem. 271*, 29009−29015.
11. Boll, W., Ohno, H., Songyang, Z., Rapoport, I., Cantley, L. C., Bonifacino, J. S., and Kirchhausen, T. (1996) *EMBO J. 15*, 5789−5795.
12. Sorkin, A., McKinsey, T., Shih, W., Kirchhausen, T., and Carpenter, G. (1995) *J. Biol. Chem. 270*, 619−625.
13. Nesterov, A., Wiley, H. S., and Gill. G. N. (1995) *Proc. Natl. Acad. Sci. U.S.A. 92*, 8719−8723.
14. van Delft, S., Schumacher, C., Hage, W., Verkleij, A. J., and van Bergen en Henegouwen, P. M. P. (1997) *J. Cell Biol. 136*, 811−821.
15. Benmerah, A., Lamaze, C., Bègue, B., Schmid, S. L., Dautry-Varsat, A., and Cerf-Bensussan, N. (1998) *J. Cell Biol. 140*, 1055−1062.
16. den Hartigh, J. C., van Bergen en Henegouwen, P. M. P., Verkleij, A. J., and Boonstra, J. (1992) *J. Cell Biol. 119*, 349−355.
17. van der Heyden, M. A. G., Nievers, M., Verkleij, A. J., Boonstra, J., and van Bergen en Henegouwen, P. M. P. (1997) *FEBS Lett. 410*, 265−268.
18. Walton, G. M., Chen, W. S., Rosenfeld, M. G., and Gill, G. N. (1990) *J. Biol. Chem. 265*, 1750−1754.

19. Countaway, J. L., Gironès, N., and Davis, R. J. (1989) *J. Biol. Chem. 264*, 13642−13647.
20. Davis, R. J. (1988) *J. Biol. Chem. 263*, 9462−9469.
21. Waterfield, M. D., Mayes, E. L. V., Stroobant, P., Bennet, P. L. P., Young, S., Goodfellow, P. N., Banting, G. S., and Ozanne, B. (1982) *J. Cell. Biochem. 20*, 149−161.
22. Countaway, J. L., Nairn, A. C., and Davis, R. J. (1992) *J. Biol. Chem. 267*, 1129−1140.
23. Aiyer, A., and Leis, J. (1993) *BioTechniques 14*, 366−368.
24. Ho, S. H., Hunt, H. D., Horton, R, M., Pullen, J. K., and Pease, L. R. (1989) *Gene 77*, 51−59.
25. Kawamoto, T., Sato, J. D., Le, A., Polikoff, J., Sato, G. H., and Mendelsohn, J. (1983) *Proc. Natl. Acad. Sci. U.S.A. 80*, 1337−1341.
26. Livneh, E., Prywes, R., Kashles, O., Reiss, N., Sasson, I., Mory, Y., Ullrich, A., and Schlessinger, J. (1986) *J. Biol. Chem. 261*, 12490−12497.
27. Theroux, S. J., Latour, D. A., Stanley, K., Raden, D. L., and Davis, R. J. (1992) *J. Biol. Chem. 267*, 16620−16626.
28. Lund, K. A., Opresko, L. K., Starbuck, C., Walsh, B. J., and Wiley, H. S. (1990) *J. Biol. Chem. 265*, 15713−15723.
29. Starbuck, C., and Lauffenburger, D. A. (1992) *Biotechnol. Prog. 8*, 132−143.
30. Sorkin, A., Waters, C., Overholser, K. A., and Carpenter, G. (1991) *J. Biol. Chem. 266*, 8355−8362.
31. Patschinsky, T., Hunter, T., Esch, F. S., Cooper, J. A., and Sefton, B. M. (1982) *Proc. Natl. Acad. Sci. U.S.A. 79*, 973−977.
32. Smart, J. E., Opperman, H., Czernilofsky, A. P., Purchio, A. F., Erikson, R. L., and Bishop, J. M. (1981) *Proc. Natl. Acad. Sci. U.S.A. 78*, 6013−6017.
33. Downward, J., Parker, P., and Waterfield, M. D. (1984) *Nature 311*, 483−485.
34. Sorkin, A., Helin, K., Waters, C. M., Carpenter, G., and Beguinot, L. (1992) *J. Biol. Chem. 267*, 8672−8678.
35. Helin, K., and Beguinot, L. (1991) *J. Biol. Chem. 266*, 8363−8368.
36. French, A. R., Sudlow, G. P., Wiley, H. S., and Lauffenburger, D. A. (1994) *J. Biol. Chem. 269*, 15749−15755.
37. Herbst, J. J., Opresko, L. K., Walsh, B. J., Lauffenburger, D. A., and Wiley, H. S. (1994) *J. Biol. Chem. 269*, 12865−12873.
38. Vinson, V. K., Archer, S. J., Lattman, E. E., Pollard, T. D., and Torchia, D. A. (1993) *J. Cell Biol. 122*, 1277−1283.
39. Schutt, C. E., Myslik, J. C., Rozycki, M. D., Goonesekere, N. C. W., and Lindberg, U. (1993) *Nature 365*, 810−816.
40. Jia, Z., Barford, D., Flint, A. J., and Tonks, N. K. (1995) *Science 268*, 1754−1758.
41. Waksman, G., Kominos, D., Robertson, S. C., Pant, N., Baltimore, D., Birge, R. B., Cowburn, D., Hanafusa, H., Mayer, B. J., Overduin, M., Resh, M. D., Rios, C. B., Silverman, L., and Kuriyan, J. (1992) *Nature 358*, 646−653.
42. Charifson, P. S., Shewchuk, L. M., Rocque, W., Hummel, C. W., Jordan, S. R., Mohr, C., Pacofsky, G. J., Peel, M. R., Rodriguez, M., Sternbach, D. D., and Consler, T. G. (1997) *Biochemistry 36*, 6283−6293.
43. Defize, L. H. K., Boonstra, J. Meisenhelder, J., Tertoolen, L. G. J., Tilley, B. C., Hunter, T., van Bergen en Henegouwen, P. M. P., Moolenaar, W. H., and de Laat, S. W. (1989) *J. Cell Biol. 109*, 2495−2507.
44. Diakonova, M., Payrastre, B., van Veltzen, A. G., Hage, W. J., van Bergen en Henegouwen, P. M. P., Boonstra, J., Cremers, F. F. M., and Humbel, B. M. (1995) *J. Cell Sci. 108*, 2499−2509.
45. Medvedeva, N. D., Alexeyev, V. Y., Tsupkima, N. V., and Nikolsky, N. N. (1994) *FEBS Lett. 356*, 299−301.
46. Rotin, D., Margolis, B., Mohammadi, M., Daly, R. J., Daum, G., Li, N., Fischer, E. H., Burgess, W. H., Ullrich, A., and Schlessinger, J. (1992) *EMBO J. 11*, 559−567.
47. Bishayee, A., Beguinot, L., and Bishayee, S. (1999) *Mol. Biol. Cell 10*, 525−536.
48. Stover, D. R., Becker, M., Liebetanz, J., and Lydon, N. B. (1995) *J. Biol. Chem. 270*, 15591−15597.
49. Sierke, S. L., Longo, G. M., and Koland, J. G. (1993) *Biochem. Biophys. Res. Commun. 191*, 45−54.
50. Luttrell, D. K., Lee, A., Lansing, T. J., Crosby, R. M., Jung, K. D., Willard, D., Luther, M., Rodriguez, M., Berman, J., and Gilmer, T. M. (1994) *Proc. Natl. Acad. Sci. U.S.A. 91*, 83−87.

BI990195R